Published in final edited form as:
Anal Chem. 1997 March 15; 69(6): 1119–1126.

Effects of Charge State on Fragmentation Pathways, Dynamics, and Activation Energies of Ubiquitin Ions Measured by Blackbody Infrared Radiative Dissociation

Rebecca A. Jockusch, **Paul D. Schnier**, **William D. Price**, **Eric. F. Strittmatter**, **Plamen A. Demirev**†, and **Evan R. Williams***
Department of Chemistry, University of California, Berkeley, California 94720

Abstract

Blackbody infrared radiative dissociation spectra of the $(M + 5H)^{5+}$ through $(M + 11H)^{11+}$ ions of the protein ubiquitin (8.6 kDa) formed by electrospray ionization were measured in a Fourier-transform mass spectrometer. The 5+ ion dissociates exclusively by loss of water and/or ammonia, whereas the 11+ charge state dissociates only by formation of complementary y and b ions. These two processes are competitive for intermediate charge state ions, with the formation of y and b ions increasingly favored for the higher charge states. The y and b ions are formed by cleavage of the backbone amide bond on the C-terminal side of acidic residues exclusively, with cleavage adjacent to aspartic acid favored. Thermal unimolecular dissociation rate constants for the dissociation of each of these charge states were measured. From the temperature dependence of these rates, Arrhenius activation parameters in the rapid energy exchange limit are obtained. The activation energies (E_a) and preexponential factors (A) for the 5+, 8+, and 9+ ions are 1.2 eV and 10^{12} s^{-1}, respectively. These values for the 6+ and 7+ ions are 0.9–1.0 eV and 10^{9} s^{-1}, and those for the 10+ and 11+ ions are 1.6 eV and 10^{16}–10^{17} s^{-1}. Thus, with the exception of the 5+ ion, the higher charge states of ubiquitin have *larger* dissociation activation energies than the lower charge states. The different A factors observed for production of y and b ions from different precursor charge states indicate that they are formed by different mechanisms, ranging from relatively complex rearrangements to direct bond cleavages. These results clearly demonstrate that the relative dissociation rates of large biomolecule ions by themselves are not necessarily a reliable indicator of their relative dissociation energies, even when similar fragment ions are formed.

Mass spectrometry has become a powerful analytical tool for solving fundamental and applied problems in biochemistry, medicine, and related fields. Formation and mass analysis of large gas-phase biomolecule ions[1,2] with molecular masses up to hundreds of megadaltons are now possible.[3] Information about the sequence,[4] locations of posttranslational modifications[5] or active sites in biomolecule complexes,[6] and gas-phase conformation[7] can be obtained by tandem mass spectrometry (MS/MS),[8] in which a precursor ion is mass selected, reacted, or dissociated, and the resulting product ions are mass analyzed. Relating dissociation products to ion structure in MS/MS experiments is greatly improved by applying detailed knowledge about dissociation mechanisms and energetics. While the reactivity and dissociation of small ions has been studied extensively,[9] much less is known about the dissociation pathways and energetics in large biomolecule ions. This is due, in part, to the much greater difficulty in applying conventional structural methods, such as spectroscopy,[10] high-pressure MS,[11] or computational chemistry,[12] to larger ions.

†Permanent address: Division of Ion Physics, ISV, Uppsala University, Uppsala, Sweden.

Several methods for preparing large ions with a controlled internal energy have been demonstrated. Photodissociation at different wavelengths can produce ions with precise internal energies, provided that both the number of photons absorbed and the initial internal energy of the ions are known.[13] By choosing chemical ionization reagents with different proton affinities, Speir and Amster[14] demonstrated that the internal energy of laser-desorbed peptide molecules could be varied. With surface-induced dissociation (SID), a method pioneered by Cooks and co-workers,[15] the energy deposited into an ion can be selected by changing the ion–surface collision energy.[16] Wysocki and co-workers[17] have used SID to produce large peptide ions with varying internal energies and have investigated the role of sequence on the relative stabilities of these ions. Glish and co-workers[18,19] have measured the kinetic energy loss of peptide ions dissociated in a magnetic sector instrument and found a strong correlation between the energy deposited into the precursor ions and the subsequent formation of a, b, and y ions.[18]

Although the average or maximum energy deposited with these excitation methods can be determined, an ion population with a distribution of internal energies that is often less well characterized is typically produced.[20] This can be due to uncertainties in either the ion energy prior to or the energy transferred by the activation process. In combination with statistical methods for modeling unimolecular kinetics, such as RRKM theory,[13,17,21] the energetics of the dissociation processes of peptide ions have been deduced.[13,17,18,21] While excellent qualitative information has been obtained, measurement of accurate quantitative values is more difficult if the ion internal energy distribution is not well characterized and if information about the dynamics of the dissociation process, often required for modeling kinetic data, is limited.

Thermal activation methods have the advantage that the internal energy distribution of an ion population can often be well characterized. The thermal unimolecular dissociation of small molecules has been studied extensively.[22] From the temperature dependence of these reactions, Arrhenius activation energies (E_a) and preexponential factors (A) can be determined. These values provide critical information about the mechanisms of unimolecular reactions. More recently, Smith and co-workers[23,24] demonstrated that electrospray-generated peptide ions can be dissociated thermally by raising the temperature of a heated metal capillary[25] in the electrospray interface, and they subsequently measured the depletion of the molecular ions of mellitin as a function of capillary temperature.[24] From these data, activation energies were obtained and found to decrease from 1.8 to 1.4 eV as the charge state increased from 3+ to 6 +. Implicit in their data analysis was the assumption that the relative dissociation kinetics can be directly related to the activation energies, i.e., that all the dissociation processes have the same Arrhenius A factor.[24] A similar instrumental approach was used by Meot-Ner et al.[26] to measure the Arrhenius parameters for dissociation of a pentapeptide leucine enkephalin and its proton-bound dimer. Activation energies of 1.66 and 2.02 eV and A-factors of $10^{15.7}$ and $10^{21.7}$ s^{-1}, respectively, were reported.[26]

Recently, we demonstrated a new thermal excitation technique for large biomolecule ions–blackbody infrared radiative dissociation (BIRD).[27–29] In BIRD, isolated ions dissociate by absorption of infrared blackbody photons emitted from the walls of a heated vacuum chamber in a Fourier-transform mass spectrometer, a method first demonstrated by McMahon and co-workers[30] with small, weakly bound clusters. Moreover, from the temperature dependence of the unimolecular dissociation rate constants, Arrhenius activation parameters in the zero-pressure limit can be obtained.[27–29,31–33] For small ions activated above the threshold dissociation energy, the dissociation rate is much faster than the rate of photon absorption and emission. Under these conditions, true dissociation threshold energies can be obtained from the measured activation energy by adding in correction factors.[31–34] However, the measured A factors reflect only the rate at which ions absorb photons and contain no information about the dissociation processes.

For larger ions, we have demonstrated that the rate at which ions absorb and emit photons can greatly exceed their dissociation rate under readily achievable experimental conditions.[28,29] This is due to the roughly linear increase in the photon absorption and emission rate with increasing ion size. In contrast, the dissociation rate for a process characterized by a given E_a and A factor is independent of ion size for ions that have a true Boltzmann distribution of energies at a given temperature. Under conditions where the absorption and emission rates greatly exceed the dissociation rate, ions equilibrate with the blackbody radiation field inside the vacuum chamber, and the internal energy of a population of ions is characterized by a Boltzmann distribution.[28,29]

The ion size for which this analysis applies depends on the relative rates of absorption, emission, and dissociation. Master equation modeling of these processes, successfully applied to small ions,[31–33] has been done to obtain insight into these processes for large ions.[29] For a model peptide $(Ala\text{-}Gly)_{64}$ (8.4 kDa), calculations indicate that ions with the most probable energy exchange ~8 eV/s with the chamber walls at 400 K (~70 “blackbody” photons/s), equivalent to exchanging the entire energy in each ion every 3 s.[29] In contrast, the measured dissociation rate for the 11+ ion of a similar size protein, ubiquitin (8.6 kDa), is ~0.0007 s^{-1} at this temperature. Thus, the exchange of energy between this ion and its surroundings occurs significantly faster than its rate of dissociation. In this “rapid energy exchange” (REX) limit, the thermal activation parameters measured at zero pressure should be the same as those measured in the traditional high-pressure limit. True dissociation threshold energies can thus be inferred directly from the measured E_a these values differ by a few kT). In contrast to small ions, the A factors of large ions in the REX limit depend only on the dissociation process and not on the rate at which ions absorb radiation.[29] Thus, information about the dynamics of the dissociation process can be obtained directly from these values.

Recently, Arrhenius activation parameters for singly and doubly protonated bradykinin and several of its analogues measured using BIRD were reported.[28] Calculations indicate that the majority of the observed dissociation processes for these ions are in the REX limit. For these structurally similar peptides, measured E_a values and A factors for the singly protonated ions ranged from 0.5 to 1.4 eV and from 10^5 to 10^{12} s^{-1}, respectively. The range of A factors indicates that similar processes, such as y or b ion formation, can have significantly different dissociation dynamics that depend on the structure of the precursor ion. Doubly protonated ions were found to have lower activation energies than their singly charged counterparts, although one exception was found. The increased dissociation rates of multiply charged ions has been widely attributed to charge–charge repulsion.[35,36] Here, BIRD spectra and Arrhenius parameters in the REX limit for the $(M + 5H)^{5+}$ through $(M + 11H)^{11+}$ ions (5+ to 11+ charge states) of the protein ubiquitin are reported. Both the E_a and A factors can vary dramatically with charge state. These results clearly show that the role of charge state and mechanisms for large biomolecule ion dissociation are more complicated than has been frequently assumed.

EXPERIMENTAL SECTION

All experimental measurements were performed on an external electrospray ionization source Fourier-transform mass spectrometer with a 2.7 T superconducting magnet. This instrument is described in detail elsewhere.[27,37] Ions from the external source are injected into the ion cell through five stages of differential pumping using a series of lenses to which static potentials are applied. Ion trapping is enhanced using N_2 collision gas introduced through a pulsed valve to a pressure ~2×10^{-6} Torr. The 6+ to 10+ ions were accumulated in the cell for times up to 12 s. This value was varied to optimize signal. Because of the relatively low abundance of the 5+ and 11+ charge states formed directly by electrospray ionization and the limited dynamic range of FTMS, these ions were isolated by accumulating all charge states in the ion cell for 3 s and then using SWIFT excitation to eject the charge states of greatest intensity (7+ to 9+).

This cycle was repeated up to five times to accumulate a sufficient number of ions in the cell prior to their subsequent final isolation and reaction. This method of ion accumulation is analogous to that done by quadrupolar axialization[38] but has the advantage that the internal energy of the isolated ions is not increased by nonthermal collisions. A mechanical shutter was open during ion accumulation and closed at all other times to prevent ions from entering the cell. After molecular ions of a given charge state were isolated, the fragmentation was measured as a function of time up to 300 s at several different temperatures, as described previously.[27,28] Data were acquired with a Finnigan Odyssey data system, using an acquisition rate of 941 kHz (*m*/*z* 90 cutoff), detection excitation sweep rate of 1100 Hz/μs, and 256K points collected. Spectra for the 5+ and 6+ charge states were also acquired with a 210 kHz acquisition rate to more readily resolve the loss of small neutral molecules from the molecular ions.

The heating and temperature control of the vacuum chamber for BIRD experiments has been described previously.[27] The temperature inside the vacuum chamber was measured using two calibrated copper–constantan thermocouples mounted on either side of the ion cell. In a separate experiment, the temperature inside the cell was measured using a thermocouple temporarily placed in the center of the cell. The temperature measured by this thermocouple was found to be within 1 °C of that measured by the thermocouples outside the cell over the temperature range of this experiment. The temperatures reported are those measured by the thermocouples outside the cell but corrected to correspond to the temperature inside the cell.

The ubiquitin sample was obtained from Sigma Chemical Co. (St. Louis, MO) and was used without further purification. Ions were formed by electrospray ionization from a 10^{-5} M ~60:40 methanol/water solution. Approximately 1% acetic acid was added to enhance production of the higher charge state ions.

RESULTS AND DISCUSSION

Fragmentation Pathways.

BIRD spectra of the 5+ through 11+ charge states of ubiquitin show significant differences in the fragmentation products, a phenomenon also observed with other dissociation methods.[39–41] The 5+ ion dissociates exclusively by consecutive loss of small neutral molecules corresponding to either water and/or ammonia; we are unable to unambiguously assign this loss. Dissociation of the 11+ ion results exclusively in formation of complementary y and b ions (Figure 1f). Both the loss of water/ammonia and formation of y and b ions are observed for intermediate charge state ions, with loss of water predominant for lower charge states and formation of y and b ions increasingly favored for higher charge states (Figure 1). Subsequent dissociation of some of the fragment ions occurs. For example, the lower charge state b ions have a high propensity to lose multiple water/ammonia molecules. Dissociation of the molecular ions that have lost water/ammonia also contributes to the abundance of the $(b - xH_2O/NH_3)^{n+}$ ions. The total water/ammonia loss from both precursor and fragment ions decreases from ~80% to ~3% for the 6+ and 11+ ions. For the 8+ ion, backbone cleavage and loss of water/ammonia are competitive and occur to a similar extent.

The y and b fragments observed for the 6+ to 11+ charge states of ubiquitin result from cleavage of the amide bond of the protein backbone between residues Asp^{58}-Tyr^{59}, Asp^{52}-Gly^{53}, Glu^{51}-Asp^{52}, Asp^{39}-Gln^{40}, Asp^{32}-Lys^{33}, and Glu^{18}-Pro^{19}. Thus, BIRD produces cleavage on the C-terminal side of acidic residues in this molecule with extraordinary specificity. A similar propensity for cleavages adjacent to acidic residues in peptides has been reported by both Martin et al.[42] and Qin and Chait.[43] As observed by Martin et al. for other molecules,[42] cleavage at aspartic acid is favored; cleavage occurs at four of the five Asp residues in this molecule, but only at two of the six Glu residues. The latter cleavages also occur adjacent to a Pro and Asp residue. Facile cleavage adjacent to Pro has been reported previously.[41] This

same fragmentation is also observed by CAD[40] and IRMPD,[39] but BIRD appears to be even more selective, i.e., dissociation occurs via fewer reaction pathways. The higher specificity of BIRD is presumably due to the longer time frame and lower energy excitation under the experimental conditions employed. These factors favor the lowest energy dissociation pathways. The majority of the fragmentation corresponds to just two or three processes for each charge state, although other processes are observed in minor (<5%) abundance for some charge states.

As observed for the dissociation of multiply protonated bio-molecules by other methods, some of the complementary fragments produced by BIRD of an isolated charge state have a distribution of charges. For instance, both y_{18}^{3+} and y_{18}^{2+} as well as their complements (b_{58}^{4+} and b_{58}^{5+}, respectively) are observed for the M^{7+} ion. This suggests the presence of different charge configurations for ions of a given charge state, the BIRD kinetics of which are indistinguishable (vide infra).

Resolution.

One disadvantage of BIRD in its current implementation is that heating the entire vacuum chamber adversely affects the background pressure. Higher pressure lowers the resolution attainable in FTMS.[44] The background pressure in these experiments at elevated temperatures was below 4×10^{-8} Torr. With the vacuum chamber at 156 °C, a resolution of 20 000 (fwhm) was obtained for the 10+ ion of ubiquitin (Figure 1e, inset), even when operating over a relatively broad bandwidth (lower mass cutoff at *m*/*z* 400) and at a relatively low magnetic field strength of 2.7 T. This is sufficient to resolve the unit mass isotopic distribution of this ion. From the *m*/*z* separation of the isotope peaks, the charge state of the ion can be readily assigned.[45] Thus, the slightly higher background pressure does not appear to be a significant impediment to extending BIRD to even larger ions.

Dissociation Kinetics.

The time dependence of ion dissociation for each charge state was investigated at several temperatures for reaction delays up to 300 s. Rate constants for dissociation at a given temperature were obtained from a linear least-squares fit of a plot of $\ln\{[M^+]/[M^+] + \sum[F^+])\}$ vs time, where $[M^+]$ and $[F^+]$ refer to the abundance of the precursor ion and fragment ions, respectively. An example of these data is shown in Figure 2 for the 7+ and 11+ ions dissociated at several different temperatures. Evidence for two different structures for the 12+ ion of ubiquitin has been recently reported.[46] The excellent fit of the BIRD data to a single rate constant indicates that any conformational or charge configurational isomers that may be present for the 5+ to 11+ ions have indistinguishable dissociation kinetics. Under the experimental conditions used, ions with charge states above 11+ were not produced with sufficient abundance to isolate and measure their BIRD kinetics. Dissociation efficiencies between 80 and 100% for each ion were achieved at longer times and higher temperatures. The efficiency of BIRD appears to be limited only by these two factors.

At the background pressure of these experiments, the collision frequency of ubiquitin ions with a neutral hydrocarbon such as butane is $<10\ s^{-1}$. Thus, many thermal collisions occur over the time frame of these experiments. As demonstrated previously,[28,29] the rate constants for dissociation of large ions, such as ubiquitin 5+ and bradykinin, are independent of pressure up to 2×10^{-7} Torr, indicating that the energy transferred by radiative processes is significantly greater than that by collisions under these conditions. This result is consistent with kinetics that are in the REX limit. Collisions can also potentially result in charge transfer reactions which would interfere with the BIRD measurements. However, only product ions attributable to precursor ion dissociation are observed for all charge states over the entire temperature range

of these experiments; no evidence of charge exchange of either precursor or fragment ions was found.

From the temperature dependence of the rate constants, Arrhenius activation parameters in the zero-pressure limit are obtained. An Arrhenius plot for the 5+ to 11+ ions is shown in Figure 3. From this plot, the relative dissociation kinetics for each of these charge states over the temperature range investigated is readily apparent. For the 5+ to 7+ ions, which dissociate primarily by loss of water/ammonia, the dissociation rates decrease with increasing charge state at all temperatures investigated. In contrast, the rates for the 8+ to 11+ ions, which dissociate to form primarily y and b ions, increase with increasing charge state. The 7+ ion dissociates more readily than the 8+ and 9+ ions at the lower temperatures. A similar observation was reported by McLafferty and co-workers using IRMPD at ambient temperature.[39]

Our kinetic measurements are carried out over a limited range of temperature (depending on charge state) to yield rate constants between 0.0020 and 0.20 s^{-1}. The most accurate kinetic data are obtained in the middle of this range. Measurements at higher temperature (higher rate constants) are complicated both by the uncertainty of whether the dissociation rate is too fast to maintain kinetics in the REX limit and by the length of time required to accumulate sufficient ions for these measurements. The latter is a function of the charge state distribution produced by the electrospray process. At lower temperatures (lower rate constants), ion loss can occur over the long time frame of the experiment (300 s). An additional complication is that product ions can also undergo subsequent dissociation. This distributes the ion signal over many different peaks, resulting in an overall loss of signal-to-noise. The combination of these factors affects the range of rate constants measured for each charge state. Over the temperature range investigated for each ion, the Arrhenius plots are linear within experimental error. This indicates both that the ion internal energy distribution is not significantly perturbed at higher temperatures and that any competing processes that may occur do not have drastically different Arrhenius parameters (vide infra).

Arrhenius Activation Energies.

From the Figure 3 data, the Arrhenius activation energy and preexponential factor for the dissociation of each charge state are obtained from the slope and *y*-intercept, respectively. These values are given in Table 1. The errors reported for the Arrhenius parameters are obtained from a linear least-squares fit of these data. These values account for random but not systematic error that may be present in this experiment. Examples of systematic error include a nonuniform vacuum chamber temperature, which would result in deviations from a Planck distribution at a given temperature, and differences in the relative detection efficiency of product vs precursor ions. The latter has been shown previously to have a large effect on the measured rate constant but a relatively small effect on the Arrhenius parameters.[28]

The E_a and A factor for the 5+, 8+, and 9+ ions are 1.2 eV and 10^{12} s^{-1}, respectively. These values are indistinguishable within experimental error, despite the clearly different dissociation kinetics for these ions. The kinetic data are highly sensitive to small differences in the Arrhenius parameters. For example, if the A factors for dissociation of the 8+ and 9+ ions were identical, a $\Delta E_a < 0.01$ eV would account for the observed difference in dissociation rates. The E_a and A factor for the 6+ and 7+ ions (0.9–1.0 eV and 10^9 s^{-1}, respectively) are clearly lower than those for the other ions. The lower E_a accounts for the higher dissociation rates observed for these ions vs those of the 8+ and 9+ ions at the lower temperatures. Formation of y_{18}^{3+}/b_{58}^{4+-6+} is the predominant y/b fragmentation process for the 7+ to 9+ ions. Loss of water/ammonia is the dominant process for the 5+ and 6+ ions, the activation parameters for which are clearly distinguishable. Thus, the precursor charge state affects this process (or processes).

The E_a and A factors for the 10+ and 11+ ions are 1.6 eV and 10^{16}–10^{17} s^{-1}, respectively, and are indistinguishable from each other within experimental error, again despite the differences in their dissociation kinetics. Both Arrhenius parameters are clearly higher than those of the lower charge state ions. The primary dissociation process in the 10+ ion is formation of y_{18}^{3+}/b_{58}^{7+}. Cleavage at this site is not observed in significant abundance in the 11+ ion. The predominant fragmentation for this ion is formation of y_{24}^{4+}/b_{52}^{7+}

The dissociation rate constants for the 11+ and 5+ ions are equal at ~143 °C. However, virtually no loss of water/ammonia is observed in the 11+ ion, and no y and b ions are observed in the 5+ ion. Thus, the process that causes the loss of water/ammonia in the 5+ ion is shut down in the 11+ ion. Similarly, the higher charge states make possible the formation of y and b ions, but apparently not by lowering the dissociation energy for these processes. This indicates that charge–charge repulsion in higher charge state ions does not necessarily lower bond dissociation energies but rather can significantly influence the dissociation energetics and dynamics, presumably by changing ion conformation and/or charge distribution.

For ions that dissociate by only one pathway, the Arrhenius parameters we measure can be unambiguously assigned to that process. This is the case for the 5+ ion, which undergoes sequential loss of water/ammonia. For the higher charge states, however, several product ions are formed via different reaction pathways. The Arrhenius parameters we measured for each of these charge states are a weighted average of all the fragmentation processes that occur. In principle, the individual parameters for each process could be obtained from the temperature dependence of each individual rate constant. However, this is made more complicated by subsequent fragmentation of product ions that remain in the cell. For example, $y_{18}^{3+}/b_{58}^{4+-7+} - xH_2O/NH_3$ ions are observed in the dissociation spectra of the 7+ to 10+ charge states. These ions could be formed through either process a or b in reaction Scheme 1.

To determine if the Arrhenius parameters for b/y fragmentation and loss of water/ammonia could be extracted from these experimental data, a maximum range for k_1 and k_2 was calculated by assuming that the b/y $- xH_2O/NH_3$ ions are formed exclusively by either pathway a or b. These rate constants were calculated by solving eqs 1a,b and 2. From these calculated rate constants,

$$\frac{k_1}{k_2} = \frac{([b/y] + [b/y - xH_2O])}{[M - xH_2O]} \quad (1a)$$

$$\frac{k_1}{k_2} = \frac{[b/y]}{([M - xH_2O] + [b/y - xH_2O])} \quad (1b)$$

$$k_{measd} = k_1 + k_2 \quad (2)$$

a range of Arrhenius parameters for these separate processes are obtained. For all ions except the 9+, the Arrhenius parameters are indistinguishable within experimental error and the assumptions described above. For the 9+ ion, the Arrhenius parameters for formation of water/ammonia and y/b fragmentation are 0.89–1.13 and 1.13–1.24 eV and $10^{7.9}$–$10^{10.7}$ and $10^{10.7}$–$10^{12.3}$ s^{-1}, respectively. The range of values reflects both the uncertainly in the reaction pathway and the experimental error. In principle, the contributions from each reaction pathway could be determined by continuously ejecting one of the intermediate ions (Scheme 1) from the cell during the reaction delay and measuring the rate of formation of b/y $- xH_2O/NH_3$ ions.

Coulombic Effects.

The influence of charge–charge repulsion on the thermodynamic stability of multiply protonated ions[35] and on their physical properties, such as proton transfer reactivity,[47,48] has been well documented. This effect is expected to be smaller for dissociation activation energies,[35] although the efficacy of dissociating high charge state ions has been attributed to the high Coulomb energy.[36] The Coulomb-repulsion-induced lowering of the dissociation energies for the 6+ and 11+ ions of ubiquitin was estimated using the "charges on a string" model of Rockwood et al.[35] In this model, charges are evenly spaced in one dimension using a separation distance of 3.6 Å per amino acid residue. Potentials are calculated by adding the sum of point charge Coulomb interactions (calculated using a dielectric constant of 1.00) to a Morse potential. For ubiquitin, the average charge spacing in the 6+ and 11+ ions is 55 and 27 Å, respectively. This may overestimate the true charge separation distance somewhat, as the charges are not likely to be evenly spaced[49] and some folding of the protein, e.g., to enhance local charge self-solvation, almost certainly occurs.[7] The Morse potential for the amide C–N bond was calculated using the vibration frequency of an amide stretch (1200 cm^{-1})[50] and a 1.5 eV well depth. The dissociation activation energy for cleavage of a backbone bond is lowered due to Coulomb repulsion by 0.06 and 0.11 eV for the 6+ and 11+ ions, respectively. This relatively simplistic analysis indicates that, even for the 11+ ion of ubiquitin, weakening of the backbone C–N bonds due to Coulomb repulsion should have only a small effect on the dissociation activation energy. Other factors clearly play a more significant role in the dissociation processes of these ions.

Dissociation Mechanisms.

The value of the *A* factor measured in these experiments provides information about the dynamics of the dissociation process. In small molecules, a value of 10^{12} s^{-1} is indicative of a simple but entropically unfavored process, such as a six-membered ring rearrangement.[22] By comparison, this suggests that formation of the y and b ions and loss of water/ammonia in the 5+, 8+, and 9+ ions could occur by relatively simple rearrangement reactions. The mechanism proposed by Martin et al.[42] for y and b ions formed by cleaving an Asp-Pro bond has the hydrogen from the side-chain carboxylic acid group rearranging to the nitrogen of the amide backbone with subsequent cleavage at this site (Figure 4; "neutral" reaction pathway b). By analogy to the values for small molecules, the *A* factor of 10^{12} s^{-1} measured here is consistent with this mechanism. The lower value observed for the 7+ ion suggests a more complicated rearrangement that is even less entropically favored. This indicates that some portion of the ion remote in connectivity, but not necessarily spatially, influences this reaction.

In contrast, the *A* factors of 10^{16}–10^{17} s^{-1} measured for the 10+ and 11+ ions are indicative of processes that are significantly more entropically favored. Values of 10^{15}–10^{17} s^{-1} are characteristic of direct bond cleavages in small molecules, with the higher values indicating a transition state with increased degrees of freedom, e.g., the dissociation opens up free rotations in the transition state.[22] The high value observed for the 10+ and 11+ ions indicates that the rearranged hydrogen, which is required for the formation of y and b ions, is located at the amide nitrogen in both the reactant and transition state ion. Although the amide nitrogen is not considered to be as basic as other sites in this ion, the basicity of this site could be dramatically increased via electrostatic interactions with the negatively charged carboxylate group of the adjacent deprotonated acidic residue. Such a salt-bridge interaction has been reported in the proton transfer intermediate of betaine and ammonia[51] and in the lowest energy structure of small peptides containing arginine residues.[27,28] Additional evidence for salt-bridge interactions, based on the dissociation products of multiply protonated peptide ions, has been recently reported.[52] Fragmentation of the amide bond in such a structure would then correspond to a direct bond cleavage and still form y and b ions (Figure 4; "salt-bridge" reaction a).

It is possible that the dissociation process goes through one or more relatively long-lived intermediates that have low activation energies of formation and that dissociation of an intermediate species is the rate-limiting step we measure. This intermediate could correspond to the proposed salt-bridge structure (Figure 4; "salt-bridge" reaction d), or even a proton-bound species in which the hydrogen rearrangement and subsequent bond cleavage have already occurred (Figure 4; "proton-bound" reaction d). Dissociation by this pathway would also have a high *A* factor similar to those of ion–molecule dissociations. We are unable to distinguish these two reaction pathways, although the lower activation energies for formation of y/b fragmentation from the lower charge state ions is less consistent with the latter mechanism.

The *A* factors for dissociation of large ions can be significantly lower than those measured for small ions.[28] These low values are consistent with more complicated dissociation processes that can occur for larger molecules with more degrees of freedom. It is also possible that *A* factors for some dissociation processes in large ions may be even larger for 10^{17} s^{-1}, so these values may not be directly comparable to those reported for small molecules. An *A* factor for the dissociation of the proton-bound dimer of leucine enkephalin of $10^{21.7}$ s^{-1} was measured by Meot-Ner et al. using a heated capillary interface.[26] This unusually high value could be the result of interference from other processes, such as ion desolvation, that also occur in this region under the experimental conditions employed. BIRD experiments have the advantage that only the temperature dependence of the fragmentation process of the isolated ion itself is measured. Additional experiments with other large molecules should provide further information on the validity of these comparisons.

CONCLUSION

Arrhenius activation parameters and fragmentation pathways measured by BIRD for the 5+ through 11+ ions of ubiquitin are reported. Lower charge states of ubiquitin preferentially lose small neutral molecules, either water and/or ammonia. Higher charge state ions dissociate primarily by formation of y and b ions, with the 5+ and 11+ ions dissociating exclusively by loss of water/ammonia and formation of y and b ions, respectively. The y and b ions occur exclusively adjacent to acidic residues, with cleavage at aspartic acid favored. The dissociation activation energies of the 10+ and 11+ ions are higher than those of the 5+ to 9+ ions. This indicates that the role of charge–charge repulsion on the dissociation energetics and dynamics of ubiquitin for higher charge state ions is not simply one of weakening the backbone bonds but rather via changing the gas-phase ion conformation and/or charge distribution.

Formation of y/b ions from the 7+ to 11+ charge states of ubiquitin have Arrhenius preexponentials ranging from 10^9 to 10^{17} s^{-1}, indicating that these product ions are formed by different mechanisms ranging from relatively complex rearrangements to direct bond cleavages. These results clearly demonstrate that, without information about the dynamics of the dissociation process, the relative dissociation rates of ions alone can be a poor indicator of the relative activation energy for dissociation, even for otherwise apparently similar processes.

BIRD appears to be a highly promising method for extracting information about the structure, energetics, and dissociation dynamics of large ions. The use of this method for measuring binding energies of specific noncovalent interactions of biomolecules in the gas phase and for elucidating the role of charge state in the dissociation of other ions is currently under investigation.

Acknowledgements

The authors are grateful for the generous financial support provided by the National Science Foundation (CHE-9258178, National Institutes of Health (IR29GM50336-01A2), Finnigan MAT through sponsorship of the 1994

American Society for Mass Spectrometry Research Award (E.R.W.), and the Uppsala University Fund for Bilateral Collaborations (P.A.D.).

References

1. Fenn JB, Mann M, Meng CK, Wong SF, Whitehouse CM. Science 1989;246:64–71. [PubMed: 2675315]Smith RD, Loo JA, Loo RRO, Busman M, Udseth HR. Mass Spectrom Rev 1991;10:359–451.
2. Hillenkamp, F.; Karas, M.; Beavis, RC.; Chait, BT. , . Anal Chem. 1991. p. 1193A-1203A.
3. Chen R, Cheng X, Mitchell DW, Hofstadler SA, Wu Q, Rockwood AL, Sherman MG, Smith RD. Anal Chem 1995;67:1159–1163.
4. O'Connor PB, Speir JP, Senko MW, Little DP, McLafferty FW. J Mass Spectrom 1995;30:88–93.McLuckey SA, Habibi-Goudarzi S. J Am Chem Soc 1993;115:12085–12095.Dongré AR, Somogyi A, Wysocki VH. J Mass Spectrom 1996;31:339–350. [PubMed: 8799282]Hunt DF, Yates JR III, Shabanowitz J, Winston S, Hauer CR. Proc Natl Acad Sci USA 1986;83:6233–6237. [PubMed: 3462691]
5. Huddleston MJ, Bean MF, Carr SA. Anal Chem 1993;65:877–884. [PubMed: 8470819]
6. Kelleher NL, Costello CA, Begley TP, McLafferty FW. J Am Soc Mass Spectrom 1995;6:981–984.Zaia J, Jiang L, Han MS, Tabb JR, Wu Z, Fabris D, Fenselau C. Biochemistry 1996;35:2830–2835. [PubMed: 8608118]
7. Wood TD, Chorush RA, Wampler FM, Little DP, O'Connor PB, McLafferty FW. Proc Natl Acad Sci USA 1995;92:2451–2454. [PubMed: 7708663]Clemmer DE, Hudgins RR, Jarrold MF. J Am Chem Soc 1995;117:10141–10142.Collings BA, Douglas DJ. J Am Chem 1996;118:4488–4489.Gross DS, Schnier PD, Rodriguez-Cruz SE, Fagerquist CK, Williams ER. Proc Natl Acad Sci USA 1996;93:3143–3148. [PubMed: 8610183]Covey T, Douglas DJ. J Am Soc Mass Spectrom 1993;4:616–623.
8. Busch, K. L.; Glish, G. L.; McLuckey, S. A. Mass Spectrometry/Mass Spectrometry: Techniques and Applications of Tandem Mass Spectrometry; VCH Publishers: New York, 1988. McLafferty, F. W. Tandem Mass Spectrometry; John Wiley and Sons: New York, 1983.
9. Bowers, M. T., Ed. Gas-Phase Ion Chemistry; Academic Press, Inc.: New York, 1979; Vols. 1 and 2.
10. Maier, J. P., Ed. Ion and Cluster Ion Spectroscopy and Structure; Elsevier: New York, 1989.
11. Kebarle P. Annu Rev Phys Chem 1977;28:445–476.
12. Hirst, D. M. A Computational Approach to Chemistry; Blackwell Scientific Publications: London, 1990. Hehre, W. J.; Radom, L.; Schleyer, P. R.; Pople, J. A. Ab Initio Molecular Orbital Theory; Wiley: New York, 1986.
13. Tecklenburg RE Jr, Miller MN, Russell DH. J Am Chem Soc 1989;111:1161–1171.
14. Speir JP, Amster IJ. J Am Soc Mass Spectrom 1995;6:1069–1078.
15. Cooks RG, Ast T, Mabud MA. Int J Mass Spectrom Ion Processes 1990;100:209–265.and references cited therein.
16. DeKrey MJ, Kenttamaa HI, Wysocki VH, Cooks RG. Org Mass Spectrom 1986;21:193–195.Pradeep T, Miller SA, Cooks RG. J Am Soc Mass Spectrom 1993;4:769–773.
17. Vékey K, Somogyi A, Wysocki VH. Rapid Commum Mass Spectrom 1996;10:911–918.
18. Vachet RW, Winders AD, Glish GL. Anal Chem 1996;68:522–526. [PubMed: 8712360]
19. Vachet RW, Asam MR, Glish GL. J Am Chem Soc 1996;118:6252–6256.
20. Vékey K. J Mass Spectrom 1996;31:445–463.
21. Griffin LL, McAdoo DJ. J Am Soc Mass Spectrom 1993;4:11–15.Marzluff EM, Campbell S, Rodgers MT, Beauchamp JL. J Am Chem Soc 1994;116:7787–7796.
22. Benson, S. W. Thermochemical Kinetics. Methods for the Estimation of Thermochemical Data and Rate Parameters; John Wiley & Sons: New York, 1968.
23. Rockwood AL, Busman M, Udseth HR, Smith RD. Rapid Commum Mass Spectrom 1991;5:582–585.
24. Busman M, Rockwood AL, Smith RD. J Phys Chem 1992;96:2397–2400.
25. Chowdhury SK, Katta V, Chait BT. Rapid Commum Mass Spectrom 1990;4:81–87.

26. Meot-Ner (Mautner) M, Dongré AR, Somogyi Á, Wysocki VH. Rapid Commum Mass Spectrom 1995;9:829–836.
27. Price WD, Schnier PD, Williams ER. Anal Chem 1996;68:859–866.
28. Schnier PD, Price WD, Jockusch RA, Williams ER. J Am Chem Soc 1996;118:7178–7189. [PubMed: 16525512]
29. Price WD, Schnier PD, Jochusch RA, Strittmatter EF, Williams ER. J Am Chem Soc 1996;118:10640–10644. [PubMed: 16467929]
30. Thölmann D, Tonner DS, McMahon TB. J Phys Chem 1994;98:2002–2004.
31. Dunbar RC, McMahon TB, Tholmann D, Tonner DS, Salahub DR, Wei D. J Am Chem Soc 1995;117:12819–12825.
32. Lin C, Dunbar RC. J Phys Chem 1996;100:655–659.
33. Price WD, Schnier PD, Williams ER. J Phys Chem 1997;101:664–673.
34. Dunbar RC. J Phys Chem 1994;98:8705–8712.
35. Rockwood AL, Busman M, Smith RD. Int J Mass Spectrom Ion Processes 1991;111:103–129.
36. Ishikawa K, Nishimura T, Koga Y, Niwa Y. Rapid Commum Mass Spectrom 1994;8:933–938.
37. Gross DS, Williams ER. J Am Chem Soc 1995;117:883–890.
38. Bruce JE, Anderson GA, Hofstadler SA, Van Orden SL, Sherman MS, Rockwood AL, Smith RD. Rapid Commun Mass Spectrom 1993;7:914–919.Bruce JE, Van Orden SL, Anderson GA, Hofstadler SA, Sherman MS, Rockwood AL, Smith RD. J Mass Spectrom 1995;30:124–133.
39. Little DP, Speir JP, Senko MW, O'Connor PB, McLafferty FW. Anal Chem 1994;66:2809–2815. [PubMed: 7526742]
40. Senko MW, Speir JP, McLafferty FW. Anal Chem 1994;66:2801–2808. [PubMed: 7978294]
41. Loo JA, Edmonds CG, Smith RD. Anal Chem 1993;65:425–438. [PubMed: 8382455]
42. Yu W, Vath JE, Huberty MC, Martin SA. Anal Chem 1993;65:3015–3023. [PubMed: 8256865]
43. Qin J, Chait BT. J Am Chem Soc 1995;117:5411–5412.
44. Marshall AG, Grosshans PB. Anal Chem 1991;63:215A–229A.
45. Henry KD, McLafferty FW. Org Mass Spectrom 1990;25:490–492.
46. Cassady CJ, Carr SR. J Mass Spectrom 1996;31:247–254. [PubMed: 8799276]
47. Schnier PD, Gross DS, Williams ER. J Am Chem Soc 1995;117:6747–6757.
48. Kaltashov IA, Fenselau C. Rapid Commum Mass Spectrom 1996;10:857–861.
49. Schnier PD, Gross DS, Williams ER. J Am Soc Mass Spectrom 1995;6:1086–1097.
50. Creighton, T. E. Proteins, 2nd ed.; W. H. Freeman & Co.: New York, 1993.
51. Campbell S, Rodgers MT, Marzluff EM, Beauchamp JL. J Am Chem Soc 1995;117:12840–12854.
52. Cox KA, Gaskell S, Morris M, Whiting A. J Am Soc Mass Spectrom 1996;7:522–531.

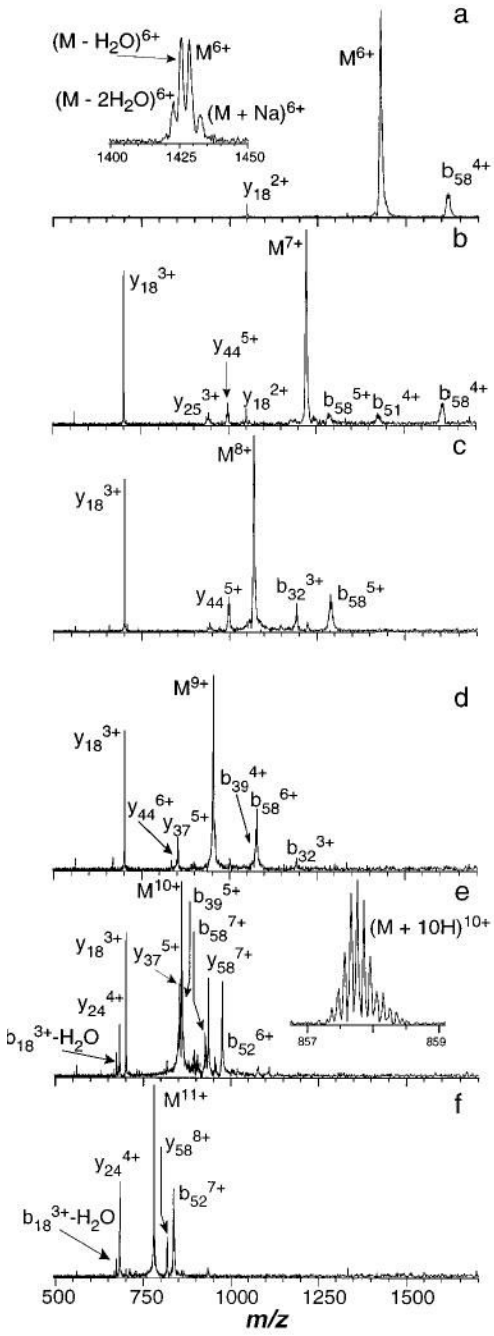

Figure 1.

Blackbody infrared radiative dissociation spectra of the 6+ to 11+ charge states of ubiquitin (a–f, respectively) taken from the kinetic data. Temperature and reaction delay for each spectrum are (a) 6+, 145 °C, 90 s; (b) 7+, 170 °C, 140 s; (c) 8+, 161 °C, 240 s; (d) 9 +, 151 ° C, 300 s; (e) 10+, 151 °C, 200 s (expansion of molecular ion at 156 °C with no reaction delay inset); and (f) 11+, 151 °C, 60 s.

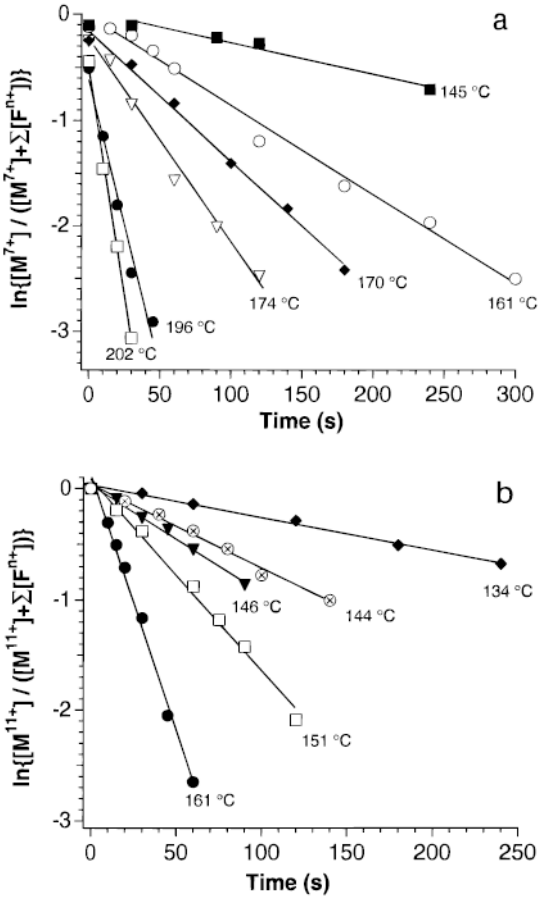

Figure 2.
Data for the dissociation of ubiquitin (a) 7+ and (b) 11+ charge states fit to first-order kinetics at the temperatures indicated.

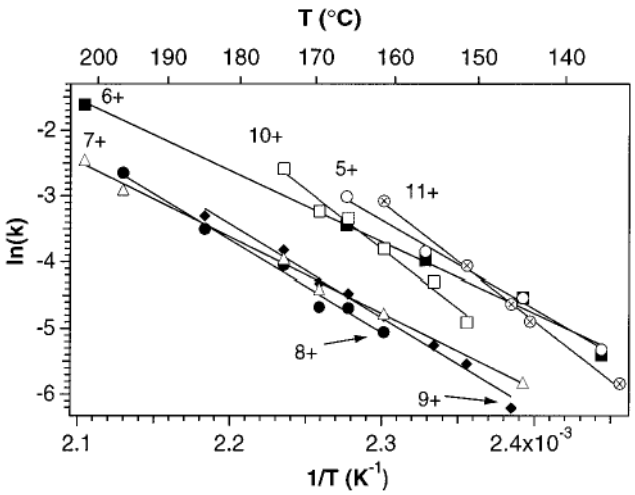

Figure 3.
Arrhenius plots for dissociation of the 5+ to 11+ charge states of ubiquitin over a temperature range of 134–202 °C.

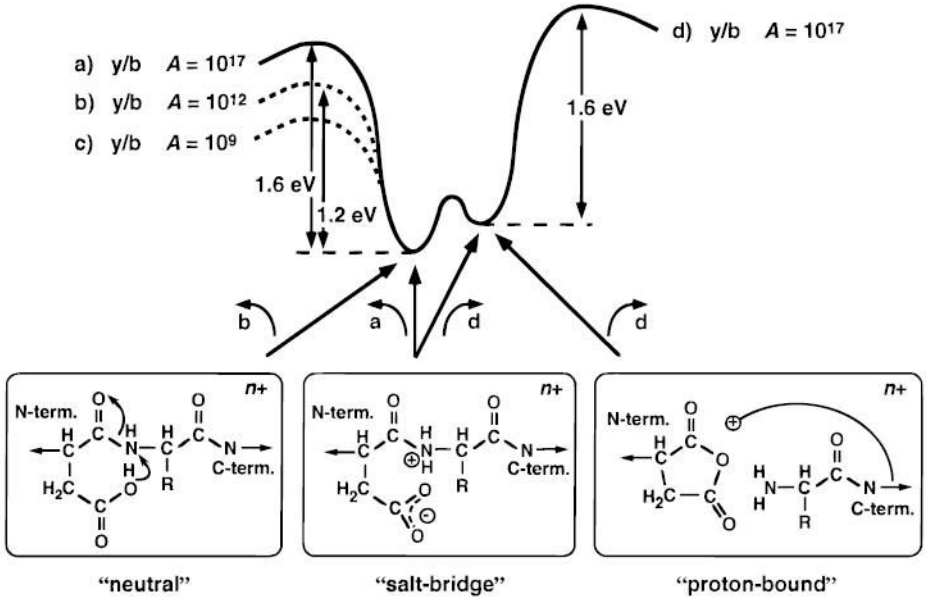

Figure 4.
Simplified reaction diagram for formation of complementary y and b ions from ubiquitin showing possible reaction pathways consistent with Arrhenius *A* factors of 10^9–10^{17} s^{-1}.

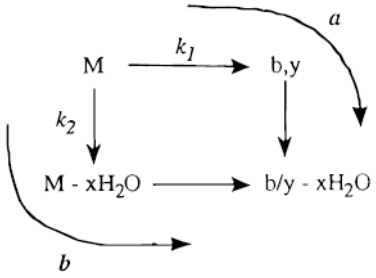

Scheme 1.

Table 1

Measured Arrhenius Activation Parameters for the 5+ through 11+ Charge States of Ubiquitin[a]

charge state	activation energy (eV)	log *A*
5+	1.16 ± 0.06	12.0 ± 0.7
6+	0.93 ± 0.04	9.2 ± 0.7
7+	0.99 ± 0.03	9.4 ± 0.3
8+	1.20 ± 0.07	11.8 ± 0.8
9+	1.21 ± 0.05	12.0 ± 0.6
10+	1.55 ± 0.11	16.3 ± 1.0
11+	1.55 ± 0.06	16.7 ± 0.7

[a]Errors are the standard deviations obtained from a linear least-squares fit of the data in Figure 3.